

## VELOCITY EFFECTS AND LOW-LEVEL FIELDS IN AXISYMMETRIC GEOMETRIES (SUMMARY OF RESULTS, PROBLEM 9)

Nathan IDA

*Department of Electrical Engineering, The University of Akron, Akron, Ohio 44325, USA*

(Received 8 March 1990)

**ABSTRACT:** A summary of results for Problem 9 of the TEAM workshop is presented in the form of a documentation of the available results. Due to unforeseen complications in the problem no comparisons have been made and the problem, with modification, will be retained for future workshops.

### INTRODUCTION

The results presented here are a summary of results for problem 9 of the TEAM Workshop [1]. Although initially intended as a comparison of results, the problem itself turned out to be more complicated than anticipated. The solution presented at the TEAM workshop in Vancouver, Canada in July 1988 [2] is the only available solution to date. This summary is, therefore, a documentation of the available results. The value of these results is in that they will be available for all who wish to compare their codes for this type of application. The problem itself will be retained for future workshops (with modifications).

### GEOMETRY AND MATERIAL PROPERTIES

The general geometry considered is shown in Fig. 1. It consists of a long tube, 28 mm in diameter (inner) and 6 mm wall thickness. The tube is made of steel or a nonmagnetic material. A relative permeability of 50 for the magnetic material and 1.0 for the nonmagnetic case are assumed. The conductivity of either material is  $5.0 \times 10^6$ . Two coils, identical in size are located 112 mm from each other (center to center) and physically connected together to allow them to move as one. Each coil is 4 mm thick and 10 mm long, as shown in Fig. 1. One coil is driven (Coil A) with an AC current at 50 Hz and a current density of  $3.0 \times 10^6$  Amp/m<sup>2</sup>. Each coil consists of 360 turns. The second coil (Coil B) is used as a pickup coil.

This problem is an important geometry in non-destructive evaluation of materials. It is extensively used in testing for corrosion on the outer surface of thick-walled ferromagnetic tubes.

The required results are the tangential and normal components of the flux density on lines L1 and L2. Specific tables were recommended for the purpose of reporting

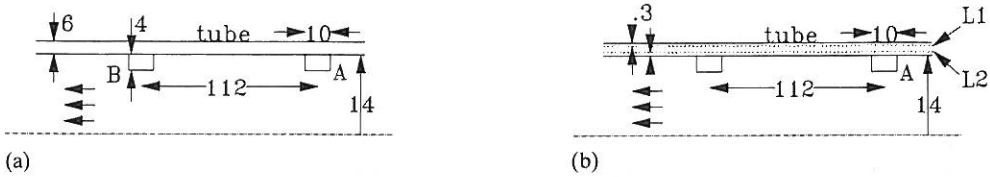


**Figure 1:** General geometry to be modeled. The geometry is axisymmetric. Arrows indicate the direction of motion. (a) Geometry. (b) Location at which the calculation of flux densities is required.

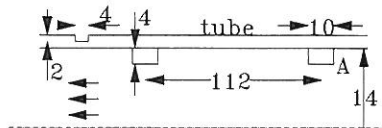


**Figure 2:** Geometry for the computation of induced voltage due to an axisymmetric slot.

[1]. These results are calculated for the magnetic and nonmagnetic materials at velocities of 0 m/s, 1 m/s and 10 m/s.

A second part of the problem is the calculation of induced voltages in coil B due to a slot (simulated defect) on the outer surface of the tube. The slot, 2 mm deep and 4 mm wide is modeled on the outer surface of the tube as shown in Fig. 2. The pickup coil (coil B) is located as shown. The induced voltage and its phase are calculated as the pickup coil moves past the slot from 15 mm from the center of the slot to 15 mm past its center.

In all cases, plotting of results is suggested although not required for comparison.

## FORMULATION AND SOLUTION

The formulation used here is an axisymmetric magnetic vector potential formulation ( $A$ ). It uses a first order quadrilateral isoparametric element. A total of 9240 elements and 9512 nodes were used. Solution time (total, rather than CPU) on a MicroVax II computer is approximately 42 minutes, using an in-core Gaussian elimination.

## RESULTS

The results presented follow the guidelines in the problem description. Results are presented in Table 1 for the ferromagnetic tube and in Table 2 for the nonmagnetic tube. Tables 1 and 2 have two parts. Table 1(a) and 2(a) are for the inner surface (line L2 in Fig. 1(b)). Table 1(b) and 2(b) are for the flux density near the outer surface (line L1 in Fig. 1(b)). In all cases the radial and axial flux densities (absolute values) are shown. Distance is measured in terms of coil diameters ( $d$ ).

Table 3 presents the induced voltage and phase angle of the induced voltage for a rectangular, circumferential slot as shown in Fig. 2. Distance is in millimeters with the center of the slot at zero distance.

**Table 1(a).** Flux densities at various locations and at different velocities for the ferromagnetic material on line L2.

	$v = 0.0 \text{ m/sec}$		$v = 1.0 \text{ m/sec}$		$v = 10.0 \text{ m/sec}$	
	$B_r$	$B_z$	$B_r$	$B_z$	$B_r$	$B_z$
0.1 d	0.171E - 02	0.114E - 02	0.172E - 02	0.123E - 02	0.173E - 02	0.132E - 02
0.5 d	0.147E - 02	0.990E - 04	0.149E - 02	0.117E - 03	0.150E - 02	0.121E - 03
1.0 d	0.122E - 03	0.708E - 05	0.125E - 03	0.890E - 05	0.127E - 03	0.915E - 05
1.5 d	0.109E - 04	0.178E - 05	0.113E - 04	0.123E - 05	0.114E - 04	0.835E - 06
2.0 d	0.108E - 05	0.147E - 05	0.108E - 05	0.632E - 06	0.103E - 05	0.836E - 07
2.5 d	0.286E - 06	0.111E - 05	0.177E - 06	0.466E - 06	0.945E - 07	0.122E - 07
3.0 d	0.199E - 06	0.868E - 06	0.947E - 07	0.352E - 06	0.919E - 08	0.388E - 08
3.5 d	0.154E - 06	0.682E - 06	0.683E - 07	0.269E - 06	0.121E - 08	0.209E - 08
4.0 d	0.121E - 06	0.537E - 06	0.511E - 07	0.206E - 06	0.338E - 09	0.131E - 08
4.5 d	0.963E - 07	0.423E - 06	0.387E - 07	0.159E - 06	0.174E - 09	0.860E - 09
5.0 d	0.769E - 07	0.333E - 06	0.296E - 07	0.123E - 06	0.109E - 09	0.575E - 09
5.5 d	0.617E - 07	0.263E - 06	0.228E - 07	0.950E - 07	0.712E - 10	0.390E - 09
6.0 d	0.497E - 07	0.206E - 06	0.176E - 07	0.736E - 07	0.489E - 10	0.267E - 09

**Table 1(b).** Flux densities at various locations and at different velocities for the ferromagnetic material on line L1.

	$v = 0.0 \text{ m/sec}$		$v = 1.0 \text{ m/sec}$		$v = 10.0 \text{ m/sec}$	
	$B_r$	$B_z$	$B_r$	$B_z$	$B_r$	$B_z$
0.1 d	0.203E - 04	0.156E - 03	0.434E - 04	0.270E - 03	0.644E - 03	0.826E - 03
0.5 d	0.628E - 04	0.900E - 04	0.127E - 03	0.132E - 03	0.499E - 03	0.105E - 03
1.0 d	0.340E - 04	0.558E - 04	0.637E - 04	0.713E - 04	0.145E - 03	0.116E - 03
1.5 d	0.212E - 04	0.420E - 04	0.368E - 04	0.498E - 04	0.523E - 04	0.630E - 04
2.0 d	0.148E - 04	0.331E - 04	0.240E - 04	0.369E - 04	0.232E - 04	0.346E - 04
2.5 d	0.109E - 04	0.264E - 04	0.168E - 04	0.281E - 04	0.118E - 04	0.202E - 04
3.0 d	0.836E - 05	0.212E - 04	0.121E - 04	0.216E - 04	0.660E - 05	0.124E - 04
3.5 d	0.651E - 05	0.171E - 04	0.898E - 05	0.167E - 04	0.391E - 05	0.787E - 05
4.0 d	0.513E - 05	0.138E - 04	0.675E - 05	0.130E - 04	0.242E - 05	0.514E - 05
4.5 d	0.408E - 05	0.112E - 04	0.513E - 05	0.102E - 04	0.155E - 05	0.342E - 05
5.0 d	0.326E - 05	0.904E - 05	0.392E - 05	0.797E - 05	0.101E - 05	0.231E - 05
5.5 d	0.262E - 05	0.730E - 05	0.302E - 05	0.624E - 05	0.674E - 06	0.158E - 05
6.0 d	0.211E - 05	0.589E - 05	0.234E - 05	0.490E - 05	0.455E - 06	0.109E - 05

**Table 2(a).** Flux densities at various locations and at different velocities for the nonmagnetic material on L2.

	$v = 0.0 \text{ m/sec}$		$v = 1.0 \text{ m/sec}$		$v = 10.0 \text{ m/sec}$	
	$B_r$	$B_z$	$B_r$	$B_z$	$B_r$	$B_z$
0.1 d	0.114E - 02	0.161E - 02	0.115E - 02	0.158E - 02	0.119E - 02	0.132E - 02
0.5 d	0.115E - 02	0.683E - 03	0.116E - 02	0.683E - 03	0.122E - 02	0.684E - 03
1.0 d	0.200E - 03	0.271E - 03	0.201E - 03	0.267E - 03	0.202E - 03	0.232E - 03
1.5 d	0.540E - 04	0.110E - 03	0.535E - 04	0.107E - 03	0.486E - 04	0.848E - 04
2.0 d	0.192E - 04	0.514E - 04	0.188E - 04	0.498E - 04	0.154E - 04	0.370E - 04
2.5 d	0.829E - 05	0.269E - 04	0.805E - 05	0.260E - 04	0.612E - 05	0.186E - 04
3.0 d	0.407E - 05	0.153E - 04	0.393E - 05	0.147E - 04	0.285E - 05	0.103E - 04
3.5 d	0.220E - 05	0.922E - 05	0.211E - 05	0.885E - 05	0.149E - 05	0.613E - 05
4.0 d	0.127E - 05	0.578E - 05	0.122E - 05	0.555E - 05	0.847E - 06	0.381E - 05
4.5 d	0.769E - 06	0.373E - 05	0.738E - 06	0.358E - 05	0.508E - 06	0.245E - 05
5.0 d	0.484E - 06	0.246E - 05	0.464E - 06	0.236E - 05	0.318E - 06	0.161E - 05
5.5 d	0.313E - 06	0.165E - 05	0.300E - 06	0.158E - 05	0.204E - 06	0.107E - 05
6.0 d	0.206E - 06	0.112E - 05	0.197E - 06	0.107E - 05	0.134E - 06	0.725E - 06

**Table 2(b).** Flux densities at various locations and at different velocities for the nonmagnetic material on L1.

	$v = 0.0 \text{ m/sec}$		$v = 1.0 \text{ m/sec}$		$v = 10.0 \text{ m/sec}$	
	$B_r$	$B_z$	$B_r$	$B_z$	$B_r$	$B_z$
0.1 d	0.248E - 03	0.837E - 03	0.538E - 03	0.751E - 03	0.609E - 03	0.833E - 03
0.5 d	0.628E - 03	0.467E - 04	0.547E - 03	0.737E - 04	0.598E - 03	0.926E - 04
1.0 d	0.194E - 03	0.135E - 03	0.164E - 03	0.129E - 03	0.165E - 03	0.144E - 03
1.5 d	0.641E - 04	0.776E - 04	0.550E - 04	0.716E - 04	0.507E - 04	0.763E - 04
2.0 d	0.252E - 04	0.418E - 04	0.219E - 04	0.385E - 04	0.188E - 04	0.395E - 04
2.5 d	0.114E - 04	0.235E - 04	0.101E - 04	0.217E - 04	0.818E - 05	0.218E - 04
3.0 d	0.579E - 05	0.139E - 04	0.515E - 05	0.129E - 04	0.405E - 05	0.127E - 04
3.5 d	0.318E - 05	0.857E - 05	0.285E - 05	0.800E - 05	0.220E - 05	0.780E - 05
4.0 d	0.186E - 05	0.546E - 05	0.168E - 05	0.511E - 05	0.128E - 05	0.495E - 05
4.5 d	0.114E - 05	0.356E - 05	0.103E - 05	0.334E - 05	0.781E - 06	0.322E - 05
5.0 d	0.720E - 06	0.236E - 05	0.654E - 06	0.222E - 05	0.494E - 06	0.213E - 05
5.5 d	0.467E - 06	0.159E - 05	0.426E - 06	0.150E - 05	0.320E - 06	0.143E - 05
6.0 d	0.309E - 06	0.108E - 05	0.282E - 06	0.102E - 05	0.211E - 06	0.970E - 06

**Table 3.** Induced voltage and phase angle for a rectangular slot. Distances are in mm.  $v$  = velocity,  $V$  = induced voltage,  $\theta$  = phase angle.

	$v = 0.0 \text{ m/sec}$		$v = 1.0 \text{ m/sec}$		$v = 10.0 \text{ m/sec}$	
	$V$	$\theta$	$V$	$\theta$	$V$	$\theta$
-15	0.60269E - 04	-0.36271E + 00	0.22216E - 04	-0.38495E - 01	0.79539E - 07	0.14143E + 01
-14	0.60535E - 04	-0.35998E + 00	0.22427E - 04	-0.35162E - 01	0.81158E - 07	0.14140E + 01
-13	0.60858E - 04	-0.35660E + 00	0.22684E - 04	-0.31050E - 01	0.83145E - 07	0.14138E + 01
-12	0.61248E - 04	-0.35240E + 00	0.22114E - 04	-0.27098E - 01	0.85586E - 07	0.14135E + 01
-11	0.61718E - 04	-0.34724E + 00	0.17192E - 04	-0.29241E - 01	0.88589E - 07	0.14132E + 01
-10	0.62282E - 04	-0.34093E + 00	0.12097E - 04	-0.37637E - 01	0.92291E - 07	0.14129E + 01
-9	0.62953E - 04	-0.33334E + 00	0.61751E - 05	-0.75730E - 01	0.96865E - 07	0.14126E + 01
-8	0.63740E - 04	-0.32435E + 00	0.55110E - 06	-0.15303E + 01	0.10253E - 06	0.14122E + 01
-7	0.64644E - 04	-0.31399E + 00	0.66979E - 05	0.10657E + 00	0.10957E - 06	0.14119E + 01
-6	0.65656E - 04	-0.30246E + 00	0.13603E - 04	0.70541E - 01	0.11836E - 06	0.14116E + 01
-5	0.66748E - 04	-0.29020E + 00	0.21826E - 04	0.58877E - 01	0.12936E - 06	0.14113E + 01
-4	0.67875E - 04	-0.27782E + 00	0.26923E - 04	0.62218E - 01	0.14316E - 06	0.14110E + 01
-3	0.68977E - 04	-0.26602E + 00	0.29497E - 04	0.70699E - 01	0.16039E - 06	0.14108E + 01
-2	0.69988E - 04	-0.25550E + 00	0.30358E - 04	0.81187E - 01	0.18145E - 06	0.14104E + 01
-1	0.70840E - 04	-0.24686E + 00	0.31083E - 04	0.89495E - 01	0.20618E - 06	0.14099E + 01
0	0.71471E - 04	-0.24059E + 00	0.31621E - 04	0.95313E - 01	0.23354E - 06	0.14091E + 01
1	0.71840E - 04	-0.23697E + 00	0.31936E - 04	0.98489E - 01	0.26185E - 06	0.14081E + 01
2	0.71919E - 04	-0.23617E + 00	0.32008E - 04	0.98947E - 01	0.28900E - 06	0.14069E + 01
3	0.71705E - 04	-0.23826E + 00	0.31831E - 04	0.96637E - 01	0.31287E - 06	0.14056E + 01
4	0.71213E - 04	-0.24316E + 00	0.31417E - 04	0.91586E - 01	0.33174E - 06	0.14044E + 01
5	0.70482E - 04	-0.25061E + 00	0.30045E - 04	0.86102E - 01	0.34455E - 06	0.14032E + 01
6	0.69570E - 04	-0.26013E + 00	0.27943E - 04	0.80221E - 01	0.35064E - 06	0.14022E + 01
7	0.68544E - 04	-0.27113E + 00	0.22898E - 04	0.82178E - 01	0.34947E - 06	0.14011E + 01
8	0.67473E - 04	-0.28289E + 00	0.19795E - 04	0.77819E - 01	0.34072E - 06	0.14000E + 01
9	0.66418E - 04	-0.29469E + 00	0.14364E - 04	0.86507E - 01	0.32475E - 06	0.13989E + 01
10	0.65428E - 04	-0.30592E + 00	0.89817E - 05	0.11119E + 00	0.30291E - 06	0.13980E + 01
11	0.64531E - 04	-0.31620E + 00	0.61336E - 05	0.13290E + 00	0.27732E - 06	0.13973E + 01
12	0.63739E - 04	-0.32535E + 00	0.10893E - 05	0.68100E + 00	0.25050E - 06	0.13970E + 01
13	0.63051E - 04	-0.33334E + 00	0.26733E - 05	-0.22941E + 00	0.22491E - 06	0.13972E + 01
14	0.62461E - 04	-0.34023E + 00	0.69608E - 05	-0.82610E - 01	0.20221E - 06	0.13979E + 01
15	0.61959E - 04	-0.34614E + 00	0.10778E - 04	-0.53267E - 01	0.18295E - 06	0.13988E + 01

In addition to these tables, the results are summarized in Figs 3–6 as plots. Figures 3 and 4 show the radial and axial components of flux density at lines L1 and L2 for the nonmagnetic and magnetic tube respectively. In each plot, the outer and inner surface flux densities (i.e. on lines L2 and L1 are shown together for comparison). All these results were calculated with zero velocity. Figures 5 and 6 show the induced voltage in the second coil due to an axisymmetric slot (Fig. 2) at zero velocity and at 10 m/sec.

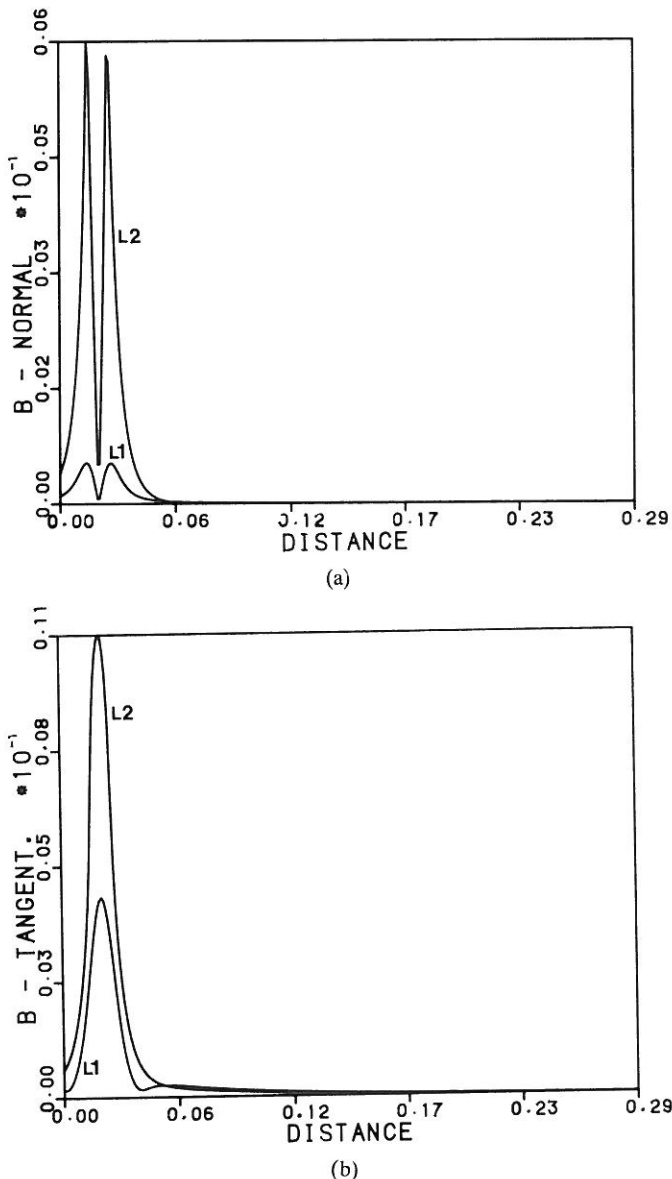


**Figure 3:** (a) Radial flux density (normal to the tube) on lines L1 and L2 (in Fig. 1(b)) for the magnetic tube. (b) Axial flux density (tangential to the tube) on lines L1 and L2 (in Fig. 1(b)) for the magnetic tube.

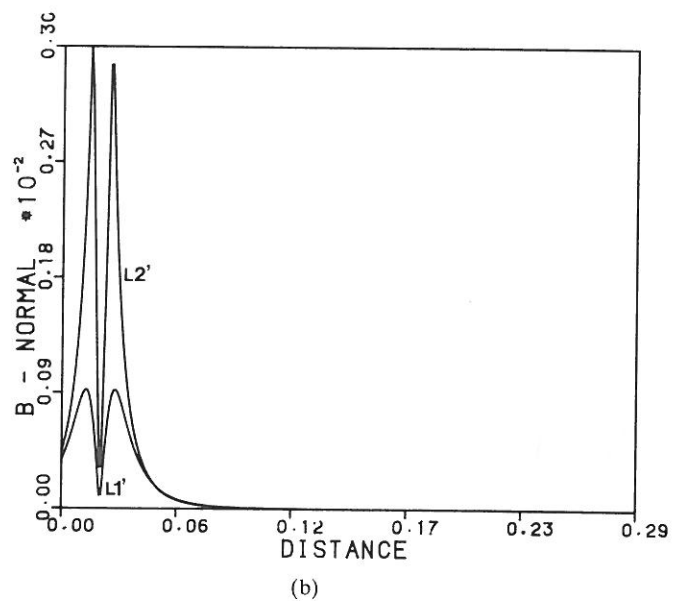
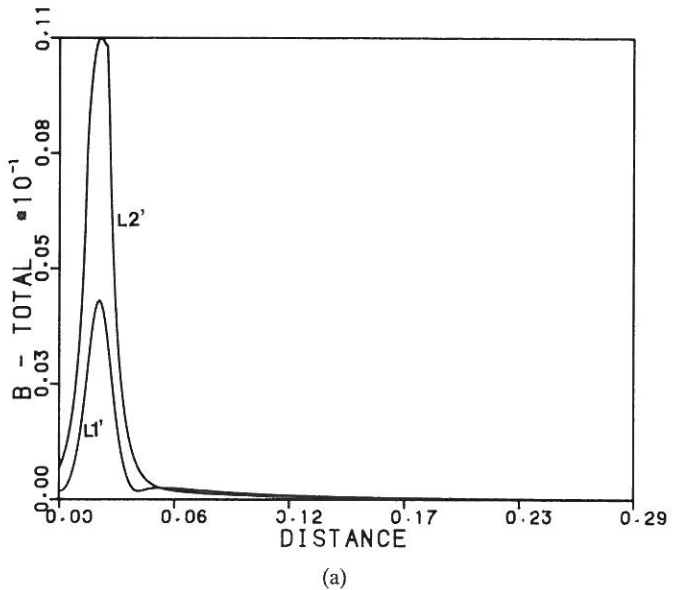


**Figure 4:** (a) Radial flux density (normal to the tube) on lines L1 and L2 (in Fig. 1(b)) for the nonmagnetic tube. (b) Axial flux density (tangential to the tube) on lines L1 and L2 (in Fig. 1(b)) for the nonmagnetic tube.

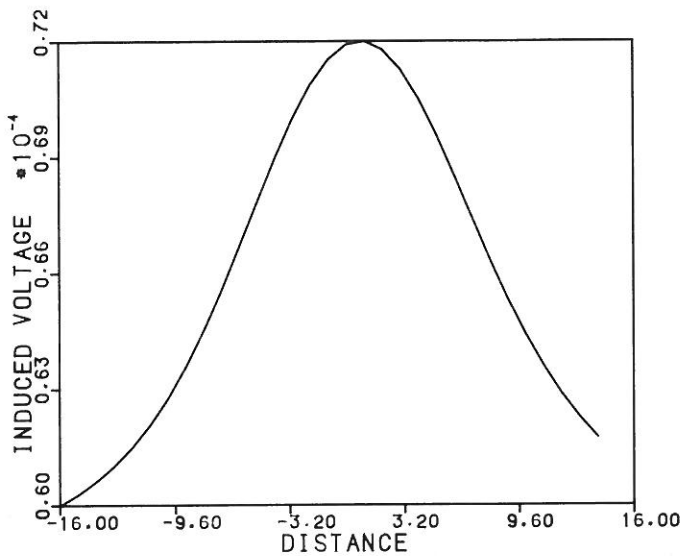


Figure 5: Induced voltage in coil  $B$  as the coil moves past the axisymmetric slot. Coil velocity is zero.

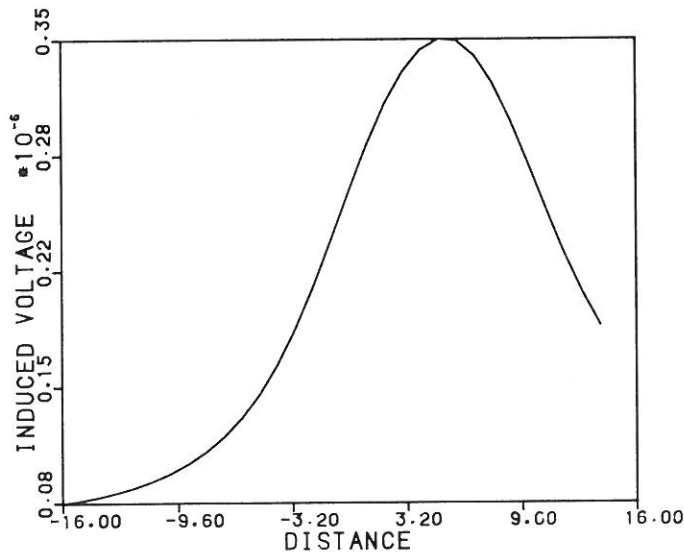
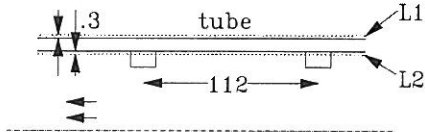


Figure 6: Induced voltage in coil  $B$  as the coil moves past the axisymmetric slot. Coil velocity is 10 m/sec.

## ADDITIONAL RESULTS

In addition to the results required in the defined problem [1], the flux densities outside the outer and inner surfaces were also calculated. These results might be more convenient for comparison with experimental results. They also indicate the actual measurements often taken in a nondestructive evaluation test. The locations



**Figure 7:** Geometry for the computation of flux densities outside the conducting (magnetic or nonmagnetic) tube. Lines L1 and L2 are 0.3 mm from the respective surfaces. All other dimensions are as in Fig. 1.

of the calculations are shown in Fig. 7. These are 0.3 mm above the outer surface and 0.3 mm below the inner surface.

Results calculated are summarized in Tables 4 and 5. These tables are similar to Tables 1 and 2. Table 4 is for the ferromagnetic tube and Table 5 for the nonmagnetic tube.

**Table 4(a).** Flux densities at various locations and at different velocities for the ferromagnetic material on line L2'.

	$v = 0.0 \text{ m/sec}$		$v = 1.0 \text{ m/sec}$		$v = 10.0 \text{ m/sec}$	
	$B_r$	$B_z$	$B_r$	$B_z$	$B_r$	$B_z$
0.1 d	0.163E - 02	0.109E - 01	0.164E - 02	0.767E - 02	0.166E - 02	0.138E - 02
0.5 d	0.138E - 02	0.195E - 02	0.141E - 02	0.153E - 02	0.142E - 02	0.259E - 03
1.0 d	0.115E - 03	0.364E - 03	0.118E - 03	0.251E - 03	0.120E - 03	0.212E - 04
1.5 d	0.103E - 04	0.192E - 03	0.107E - 04	0.109E - 03	0.108E - 04	0.199E - 05
2.0 d	0.104E - 05	0.141E - 03	0.103E - 05	0.735E - 04	0.974E - 06	0.732E - 06
2.5 d	0.302E - 06	0.110E - 03	0.181E - 06	0.541E - 04	0.892E - 07	0.428E - 06
3.0 d	0.214E - 06	0.868E - 04	0.101E - 06	0.408E - 04	0.875E - 08	0.252E - 06
3.5 d	0.166E - 06	0.692E - 04	0.734E - 07	0.311E - 04	0.119E - 08	0.155E - 06
4.0 d	0.130E - 06	0.554E - 04	0.549E - 07	0.239E - 04	0.354E - 09	0.993E - 07
4.5 d	0.104E - 06	0.445E - 04	0.417E - 07	0.184E - 04	0.186E - 09	0.654E - 07
5.0 d	0.827E - 07	0.358E - 04	0.319E - 07	0.143E - 04	0.116E - 09	0.438E - 07
5.5 d	0.664E - 07	0.289E - 04	0.245E - 07	0.111E - 04	0.764E - 10	0.298E - 07
6.0 d	0.534E - 07	0.233E - 04	0.189E - 07	0.860E - 05	0.524E - 10	0.204E - 07

**Table 4(b).** Flux densities at various locations and at different velocities for the ferromagnetic material on line L1'.

	$v = 0.0 \text{ m/sec}$		$v = 1.0 \text{ m/sec}$		$v = 10.0 \text{ m/sec}$	
	$B_r$	$B_z$	$B_r$	$B_z$	$B_r$	$B_z$
0.1 d	0.205E - 03	0.468E - 02	0.380E - 03	0.815E - 02	0.326E - 02	0.181E - 01
0.5 d	0.270E - 03	0.856E - 03	0.494E - 03	0.118E - 02	0.848E - 03	0.245E - 02
1.0 d	0.459E - 04	0.260E - 03	0.764E - 04	0.625E - 03	0.455E - 04	0.250E - 02
1.5 d	0.190E - 04	0.254E - 03	0.276E - 04	0.552E - 03	0.587E - 05	0.132E - 02
2.0 d	0.124E - 04	0.200E - 03	0.164E - 04	0.410E - 03	0.518E - 05	0.714E - 03
2.5 d	0.907E - 05	0.156E - 03	0.113E - 04	0.305E - 03	0.290E - 05	0.414E - 03
3.0 d	0.692E - 05	0.122E - 03	0.813E - 05	0.230E - 03	0.163E - 05	0.253E - 03
3.5 d	0.539E - 05	0.967E - 04	0.602E - 05	0.175E - 03	0.967E - 06	0.160E - 03
4.0 d	0.425E - 05	0.769E - 04	0.452E - 05	0.134E - 03	0.597E - 06	0.104E - 03
4.5 d	0.337E - 05	0.614E - 04	0.343E - 05	0.103E - 03	0.380E - 06	0.695E - 04
5.0 d	0.270E - 05	0.491E - 04	0.263E - 05	0.794E - 04	0.249E - 06	0.469E - 04
5.5 d	0.216E - 05	0.396E - 04	0.202E - 05	0.614E - 04	0.166E - 06	0.320E - 04
6.0 d	0.174E - 05	0.322E - 04	0.157E - 05	0.476E - 04	0.112E - 06	0.221E - 04

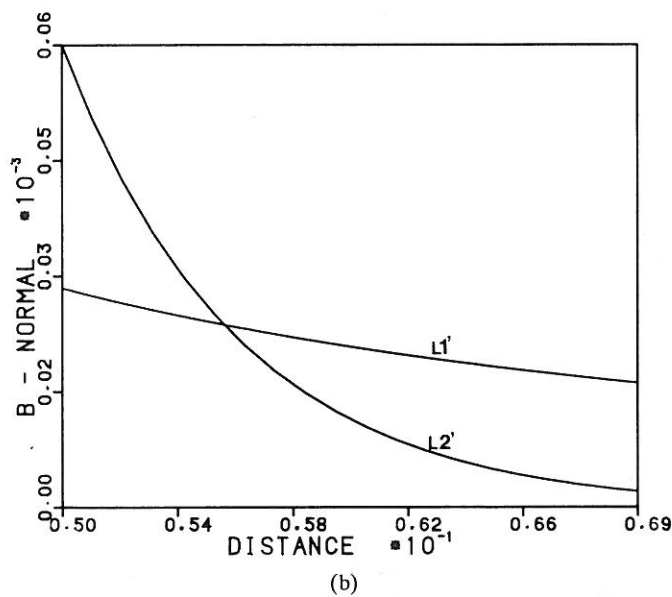
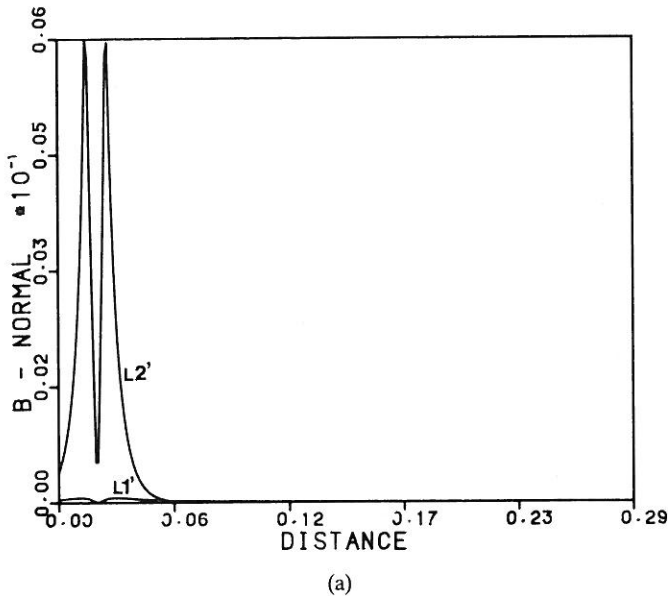
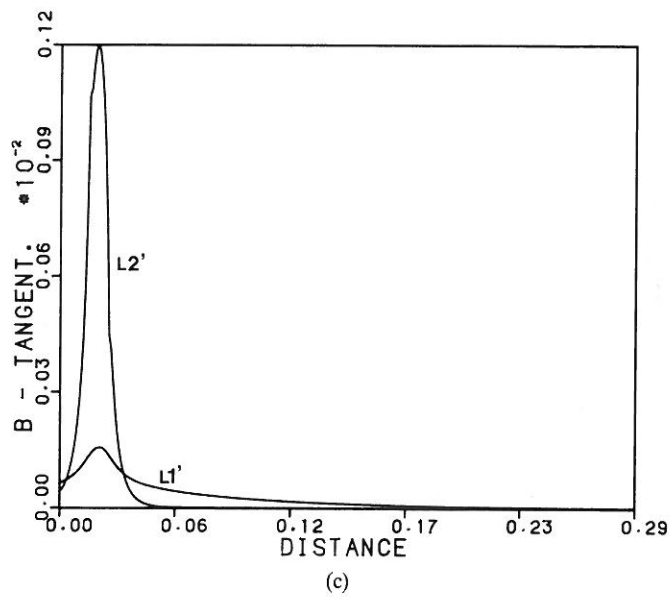
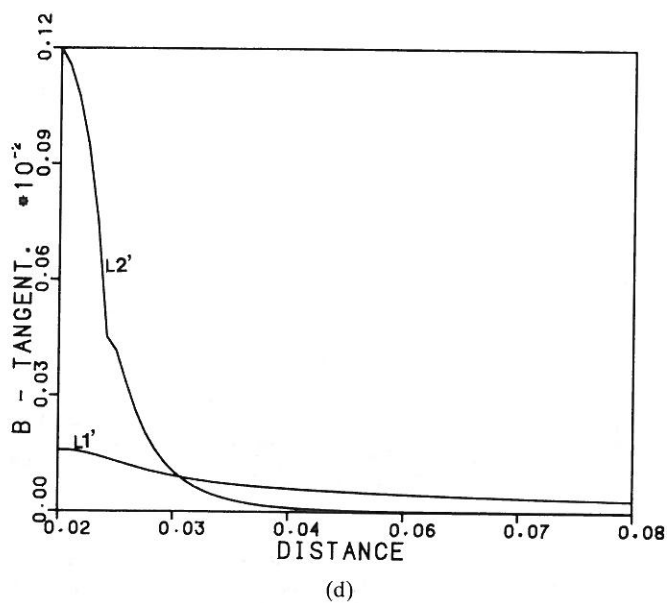


**Figure 8:** (a) Radial flux density (normal to the tube) on lines L1' and L2' (in Fig. 7) for the magnetic tube. (b) Expanded view of Fig. 8(a). The flux density on line L1' is larger than on L2'. (c) Axial flux density (tangential to the tube) on lines L1' and L2' (in Fig. 7) for the magnetic tube. (d) Expanded view of Fig. 8(c). The flux density on line L1' is larger than on L2'.



(c)



(d)

**Figure 8:** Contd.

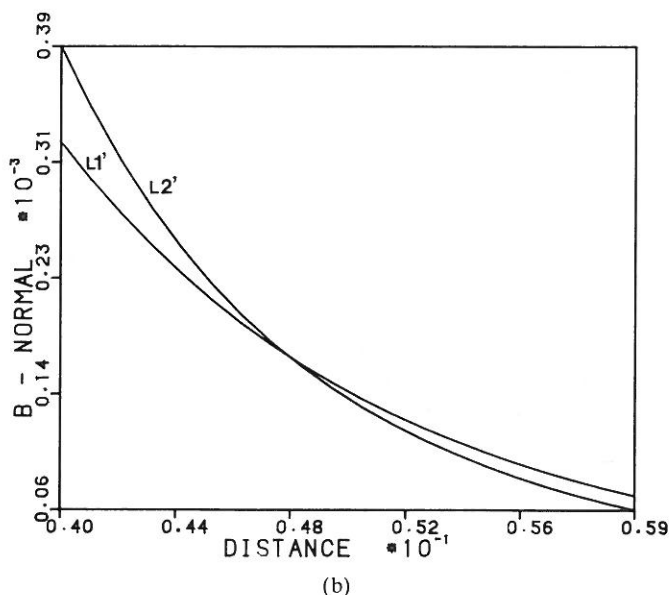
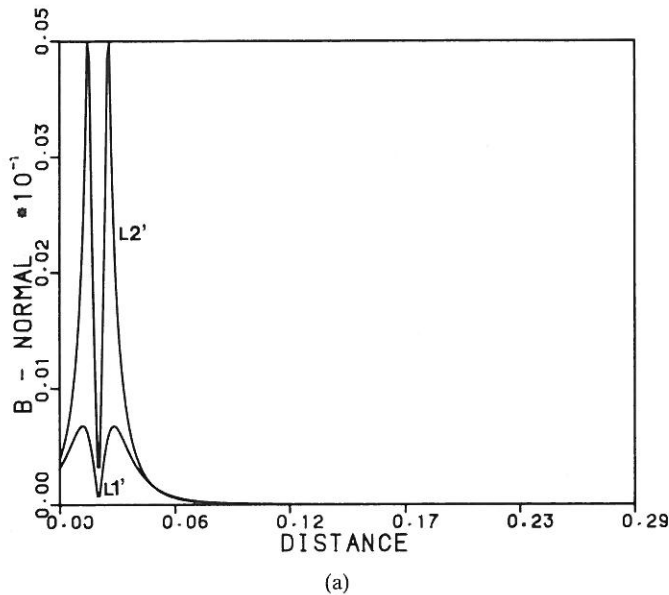


**Figure 9:** (a) Radial flux density (normal to the tube) on lines L1' and L2' (in Fig. 7) for the nonmagnetic tube. (b) Expanded view of Fig. 9(a). The flux density on line L1' is larger than on L2'.

**Table 5(a).** Flux densities at various locations and at different velocities for the nonmagnetic material on line L2'.

	$v = 0.0 \text{ m/sec}$		$v = 1.0 \text{ m/sec}$		$v = 10.0 \text{ m/sec}$	
	$B_r$	$B_z$	$B_r$	$B_z$	$B_r$	$B_z$
0.1 d	0.999E - 03	0.276E - 02	0.100E - 02	0.273E - 02	0.105E - 02	0.252E - 02
0.5 d	0.110E - 02	0.514E - 03	0.111E - 02	0.515E - 03	0.118E - 02	0.520E - 03
1.0 d	0.204E - 03	0.249E - 03	0.204E - 03	0.246E - 03	0.205E - 03	0.216E - 03
1.5 d	0.564E - 04	0.105E - 03	0.558E - 04	0.103E - 03	0.504E - 04	0.829E - 04
2.0 d	0.203E - 04	0.501E - 04	0.199E - 04	0.486E - 04	0.162E - 04	0.370E - 04
2.5 d	0.881E - 05	0.265E - 04	0.855E - 05	0.256E - 04	0.649E - 05	0.188E - 04
3.0 d	0.434E - 05	0.151E - 04	0.420E - 05	0.146E - 04	0.304E - 05	0.105E - 04
3.5 d	0.235E - 05	0.913E - 05	0.226E - 05	0.879E - 05	0.160E - 05	0.627E - 05
4.0 d	0.136E - 05	0.574E - 05	0.130E - 05	0.552E - 05	0.906E - 06	0.391E - 05
4.5 d	0.825E - 06	0.371E - 05	0.791E - 06	0.357E - 05	0.545E - 06	0.251E - 05
5.0 d	0.519E - 06	0.245E - 05	0.498E - 06	0.235E - 05	0.341E - 06	0.165E - 05
5.5 d	0.336E - 06	0.164E - 05	0.322E - 06	0.158E - 05	0.219E - 06	0.110E - 05
6.0 d	0.221E - 06	0.111E - 05	0.212E - 06	0.107E - 05	0.144E - 06	0.746E - 06

**Table 5(b).** Flux densities at various locations and at different velocities for the nonmagnetic material on line L1'.

	$v = 0.0 \text{ m/sec}$		$v = 1.0 \text{ m/sec}$		$v = 10.0 \text{ m/sec}$	
	$B_r$	$B_z$	$B_r$	$B_z$	$B_r$	$B_z$
0.1 d	0.314E - 03	0.101E - 02	0.680E - 03	0.888E - 03	0.767E - 03	0.963E - 03
0.5 d	0.705E - 03	0.512E - 04	0.600E - 03	0.113E - 03	0.654E - 03	0.136E - 03
1.0 d	0.198E - 03	0.152E - 03	0.167E - 03	0.143E - 03	0.167E - 03	0.155E - 03
1.5 d	0.635E - 04	0.824E - 04	0.543E - 04	0.754E - 04	0.494E - 04	0.780E - 04
2.0 d	0.246E - 04	0.433E - 04	0.213E - 04	0.397E - 04	0.179E - 04	0.396E - 04
2.5 d	0.111E - 04	0.241E - 04	0.972E - 05	0.222E - 04	0.772E - 05	0.216E - 04
3.0 d	0.557E - 05	0.141E - 04	0.494E - 05	0.131E - 04	0.380E - 05	0.125E - 04
3.5 d	0.305E - 05	0.869E - 05	0.273E - 05	0.808E - 05	0.205E - 05	0.765E - 05
4.0 d	0.178E - 05	0.552E - 05	0.160E - 05	0.515E - 05	0.119E - 05	0.484E - 05
4.5 d	0.109E - 05	0.359E - 05	0.983E - 06	0.336E - 05	0.726E - 06	0.315E - 05
5.0 d	0.688E - 06	0.238E - 05	0.623E - 06	0.223E - 05	0.458E - 06	0.208E - 05
5.5 d	0.446E - 06	0.160E - 05	0.405E - 06	0.150E - 05	0.297E - 06	0.140E - 05
6.0 d	0.295E - 06	0.109E - 05	0.268E - 06	0.102E - 05	0.196E - 06	0.947E - 06

Results are also summarized in Figs 8 and 9 as plots. One interesting aspect of these plots is shown in Figs 8(b), 8(d), and 9(b). While close to the coil, the flux density on or near the outer surface of the tube is lower than on the inner surface, further away the flux density on the inner surface is lower. The crossover point in each of these figures clearly indicates this. This effect is called the Far Field Effect or the Remote Field Effect and is used extensively in non-destructive testing of tubulars.

## REFERENCES

- [1] N. Ida, Velocity effects and low level fields in axisymmetric geometries, Proceedings of the Vancouver Team Workshop at the University of British Columbia, ANL/FPP/TM-230 (1988) 54–70.
- [2] TEAM Workshops: Test Problems, April 1988, Corrections in Proceedings of the Vancouver Team Workshop at the University of British Columbia, ANL/FPP/TM-230 (1988).



THE INTERNATIONAL JOURNAL FOR  
COMPUTATION AND MATHEMATICS IN  
ELECTRICAL AND ELECTRONIC  
ENGINEERING

*published quarterly in March, June, September and December by James & James,  
75 Carleton Road, London N7 0ET, UK.  
Telephone (+44) 71 607 1079 Fax (+44) 71 700 0218*

---

**ISSN 0332-1649**

#### **AIMS AND SCOPE**

Compel exists for the discussion and dissemination of numerical and analytical methods in all areas of electrical and electronic engineering. The main emphasis of the papers is on the methods. Applications of methods to particular engineering problems may be given to illustrate their use in practice.

All submissions of papers relevant to the journal are welcomed, particularly those from people or departments that have not submitted papers before. Papers should be sent to COMPEL, c/o James & James, 75 Carleton Road, London N7 0ET, UK.

Reprinted from

**COMPEL**  
THE INTERNATIONAL JOURNAL FOR  
COMPUTATION AND MATHEMATICS  
IN ELECTRICAL AND ELECTRONIC  
ENGINEERING

---

VOLUME 9 NUMBER 3 SEPTEMBER 1990

Managing Editor:

J.J.H. MILLER, Dublin, Ireland